


A critical examination of corrosion rate measurement techniques applied to reinforcing steel in concrete

Andrew Fahim¹  | Pouria Ghods¹ | O. Burkan Isgor² | Michael D.A. Thomas³

¹ Giatec Scientific, 245 Menten Place #300, Nepean, ON, Canada K2H 9E8

² Civil and Construction Engineering, Oregon State University, 101 Kearney Hall, Corvallis 97331, Oregon, USA

³ Department of Civil Engineering, University of New Brunswick, 17 Dineen Drive, Fredericton, N.B., Canada E3B 5A3

Correspondence

Andrew Fahim, Giatec Scientific, 245 Menten Place #300, Nepean, ON, Canada K2H 9E8.

Email: andrew@giatec.ca

Funding information

National Science and Engineering Research Council of Canada

This paper presents an investigation of five corrosion-monitoring techniques for reinforced concrete. The techniques studied are the potentiodynamic, galvanostatic, and coulometric direct-current techniques as well as electrochemical impedance spectroscopy (EIS), and the connectionless electrical pulse response analysis (CEPRA) technique. The study included monitoring corrosion rates on reinforced concrete specimens with a range of admixed chloride percentages, cover depths, and rebar diameters for 8 months. After this period, the rebars were extracted for mass loss measurements to determine the average corrosion rates. EIS was found to provide accurate measurements of active and passive corrosion rates with a simplified spectrum-analysis procedure. Galvanostatic and potentiodynamic techniques were able to measure the corrosion rates for actively corroding reinforcements accurately, while the coulometric technique overestimated it. For passive reinforcements, the coulometric technique provided reliable corrosion rate estimates, while the potentiodynamic technique provided a minor overestimation, due to the fast scan rate used, and the galvanostatic technique failed in detecting passivity, due to the short measurement duration and confinement failure. Finally, the CEPRA technique provided accurate corrosion rate predictions except for passive rebars with small diameters embedded in saturated concrete.

KEYWORDS

CEPRA, connectionless corrosion monitoring, electrochemical corrosion monitoring, electrochemical impedance spectroscopy, linear polarization resistance, rebar corrosion

1 | INTRODUCTION

Corrosion of reinforcing steel is one of the most prominent causes of premature concrete deterioration in North America^[1] and many parts of the world.^[2] The high pH provided by the concrete pore solution promotes the formation of a passive oxide layer that can limit the corrosion rate to insignificant values.^[3–5] However, due to pH-reducing reactions, such as carbonation, or the presence of chlorides in concentrations larger than a critical

threshold, the passive film can breakdown and active corrosion can initiate. After corrosion initiation, accurate determination of the corrosion rate is necessary in assessing structural safety, predicting service-life, or scheduling maintenance operations.

A number of electrochemical techniques can be used to measure the corrosion rate of steel in concrete. These techniques are based on the assumption that there is a linear relationship between a small polarization ($\Delta E < 20$ mV) around the open-circuit potential and the corresponding

current (ΔI); such that $R_p = \Delta E / \Delta I$, where R_p is called the polarization resistance. Once R_p is determined, the corrosion current density of reinforcement in concrete, i_{corr} , can be estimated using the Stern–Geary equation^[6]:

$$i_{\text{corr}} = \frac{\beta}{AR_p} \quad (1)$$

where A is the polarized surface area of the reinforcement and β is the Tafel constant which depends on the kinetic parameters of the corrosion process.^[6]

In theory, the value of R_p can be determined using direct current (DC) measurements or alternating current (AC) impedance spectra. Potentiodynamic^[7] and galvanostatic pulse^[8,9] techniques are the most widely used DC methods for field measurements of steel corrosion rate in reinforced concrete elements. The AC impedance technique^[10–13] requires the recording of impedance in a range from very high to low frequencies, a process that needs long measurement times during which corrosion potential may not remain stable. In addition, interpretation of the AC impedance spectra can be difficult and subjective for unspecialized professionals; therefore, it is mainly used in laboratory investigations.

Although all of these techniques are based on the determination of polarization resistance, they may yield different corrosion rates in practice because of the differences in measurement approaches and inherent assumptions.^[9,14,15] It has been shown that all of these techniques have the ability to predict polarization resistance reasonably well in laboratory settings, provided that specific testing requirements are met.^[7] In laboratory setups, the specimens are rather small and the polarized area of reinforcement is confined, small, and known. In the field, the polarized surface area of reinforcement is typically large and unconfined due to complex reinforcement detailing; therefore, accurate determination of polarization resistance is rather challenging.^[9] The main challenges in determining the corrosion rate of embedded reinforcement in concrete structures in the field can be summarized as follows:

1. Typical reinforced concrete members are large in scale (compared to typical laboratory specimens) and contain dense reinforcement detailing; therefore, the polarization takes place over an area that is hard to predict or control. Existing methods assume that the polarized area, A , is a device-specific constant that is controlled by current confinement techniques such as guard rings. However, it has been demonstrated that the polarized area is generally different from the area assumed by these devices and attempts to control the polarized area by confinement techniques have proven to be largely ineffective.^[9,16]
2. The Stern and Geary equation was derived based on the mixed-potential theory^[6,17] and assumes the occurrence of uniform corrosion on the surface of the working electrode (i.e., the rebar). However, this equation has been used by commercial devices that are implemented to measure localized corrosion rates of steel. In such cases, the correlation between measured and actual corrosion rates is expected to be highly affected by the anode size and location, anode-to-cathode surface area ratio, and concrete resistivity, among other factors.^[18]
3. The assumption that there exists a linear relationship between the applied polarization (ΔE) and the corresponding current (ΔI) might not always be correct, particularly for cases in which the potential shift is not controlled as in the case of the galvanostatic pulse technique.
4. Measurement durations and scan rates can affect the polarization resistance obtained by these techniques considerably. For example, galvanostatic pulse technique might provide significant errors when short measurement durations are used because the potential shift measured in such durations (before reaching quasi-steady-state conditions) is not only related to the polarization resistance but also the double-layer capacitance at the electrode surface.^[19]
5. A number of different methods can be used to compensate for ohmic resistance (commonly known as IR-drop). Such methods are not standardized and have generally been shown to have limitations and provide different estimates of the ohmic resistance when compared to each other.^[20,21]

In addition to these challenges, these techniques also have practical limitations in the field; therefore, they are rarely used in field applications. Some of these practical challenges include the need to establish a connection to the rebar network, which in turn requires damaging the concrete cover, and the long measurement time required by some techniques, which limits the number of measurements that can be taken from a given structure.

In recent years, several studies have reported that the reinforcement network can be polarized through the application of an external polarization without rebar connection, similar to the approach used in Wenner array probe measurements for concrete resistivity.^[22–26] These studies have shown that if an AC current is applied from the two outer probes, in a wide range of frequencies, the frequency-dependent characteristics of the interface are reflected in the complex ratio of potential difference, between the inner electrodes, to the applied current. However, the data obtained from such measurements do not directly represent the actual impedance of the system.^[23,25,27,28] The obtained results are affected by the relative direction between the Wenner array and the reinforcing bar, probe spacing, concrete cover depth, and concrete resistivity. The applied current is partially

dissipated in concrete, but some of it also polarizes the reinforcement. The current polarizing the reinforcement depends on the aforementioned factors and cannot be directly determined. Furthermore, the obtained potential difference between the two inner probes, in such a setup, is not directly related to the potential shift exhibited by the working electrode. To resolve these issues, additional analysis of the collected data is required. Recently, a new approach has been proposed to obtain corrosion rates, without the need for rebar connection and long measurement times, using a Wenner probe that is located on the surface of the concrete along the reinforcement.^[29–31] One of the objectives of this paper is to compare this approach with other well-established techniques.

This paper reports results from an experimental study to compare the corrosion rates obtained from the existing methods typically used for reinforced concrete elements and average corrosion rates obtained using gravimetric measurements following the ASTM G01^[32] procedure, and to critically analyze the reasons for the observed differences. The techniques investigated in this study are the potentiodynamic, galvanostatic, and coulstatic direct-current techniques, electrochemical impedance spectroscopy (EIS), and the newly developed connectionless electrical pulse response analysis (CEPRA) technique.

2 | EXPERIMENTAL STUDY

2.1 | Materials and specimens

A total of 16 reinforced concrete blocks (surface area = $300 \times 300 \text{ mm}^2$; depth = 100 mm) were cast for testing. As shown in Figure 1, each block was reinforced with two black steel rebars at the same cover thickness. The blocks were produced with Type GU ordinary portland cement (265 kg/m^3), 5–20 mm siliceous gravel (1055 kg/m^3) and natural river sand (940 kg/m^3) at a water-to-cement ratio (w/c) of 0.62. This ratio was selected to yield concrete with

relatively high porosity and low electrical resistance to produce sufficient amount of mass loss due to corrosion in a short period. The blocks were prepared in groups of four based on their admixed chloride content to obtain specimens with different concrete resistivity and corrosion activity and to resemble a range of field cases. The chloride dosages, admixed in the form of NaCl, were 0, 1.5, 3, and 6% chlorides by weight of cement. Three blocks in each admixed-chloride group were reinforced with 10 M (nominal diameter = 11.3 mm) rebars placed at different cover depths; that is, each block had two rebars at either 20, 40, or 70 mm cover depth. The fourth block in each group was reinforced with 20 M (nominal diameter = 19.5 mm) rebars placed at 40 mm cover depth to investigate the role of reinforcement area on corrosion rate.

Type 316 stainless steel screws were drilled at the ends of the rebars to allow for a connection between the reinforcement and the corrosion-monitoring devices. The bars were then sand blasted to remove any prior corrosion products and most of the mill scale. As shown in Figure 1, the surfaces of the rebars from 30 mm from the ends were epoxy-coated in order to prevent galvanic corrosion between the rebar and the stainless steel screw and atmospheric corrosion of the reinforcement protruding from concrete. All bars were weighed to the nearest 0.01 g. It should be noted that the interface between epoxy-coated and uncoated bar surfaces is known to be vulnerable to crevice corrosion.^[33] Therefore, the corrosion rate measurements were taken away from the interface between epoxy-coated and uncoated surfaces (at the middle of the specimen) to decrease the influence of potential crevice corrosion on the measured corrosion rates. Post-experiment inspection of the bars showed that minor crevice corrosion under the epoxy coating was present only for a few cases.

Concrete was cast in accordance with ASTM C192^[34] in two layers, with each layer tamped for 30 times. The surface was finished using a steel trowel, and specimens were covered with wet burlap and wrapped in plastic for 24 h. Specimens

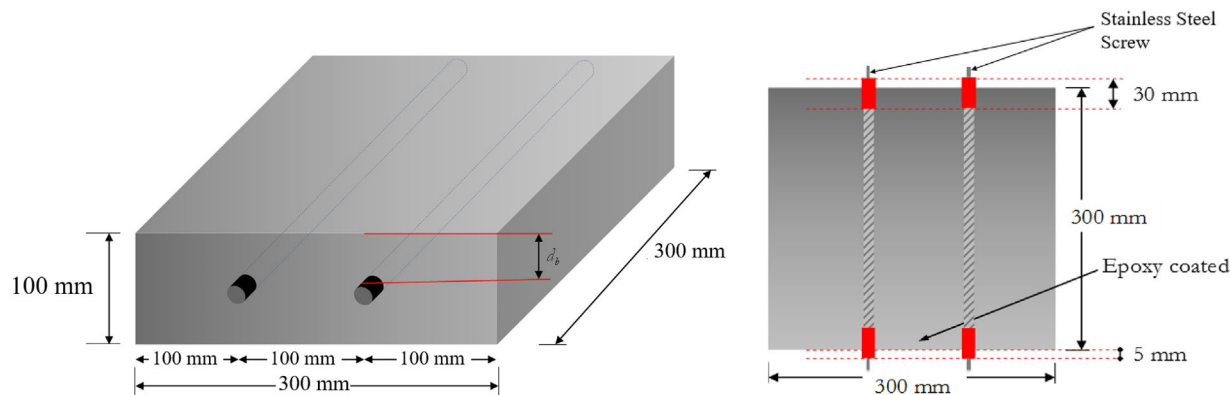


FIGURE 1 Schematic representation of the test blocks [Color figure can be viewed at wileyonlinelibrary.com]

were then removed from the formwork after 1 day, and placed on raisers in a sealed container with an approximately 30-mm-deep layer of water to ensure the availability of the required moisture and oxygen for corrosion initiation and propagation.

2.2 | Methods

The following five techniques were used in this study to monitor corrosion rates: galvanostatic pulse technique,^[8,9] potentiodynamic technique,^[7,35] coulometric technique,^[36,37] electrochemical impedance spectroscopy (EIS),^[12,13] and the CEPA technique.^[29–31] The details of these techniques can be found in the references provided; therefore, only limited and relevant information is presented in this paper.

The galvanostatic pulse technique relies on obtaining the polarization resistance through analyzing the potential response generated after the application of a known direct current pulse. The polarization resistance is obtained through fitting the experimentally obtained potential response to the response of an equivalent Randles circuit exposed to the same pulse.^[8,9,14,15] In order to limit the polarized area of reinforcement during the application of the galvanostatic pulse, an auxiliary electrode (also known as the guard-ring electrode) is used to surround the counter electrode and apply a current of a typically larger magnitude in an attempt to confine the polarizing current to an area under the counter electrode. It is postulated that the current applied from the guard ring tends to repel and confine the current from the central counter electrode to an area located under the counter electrode. In this study, a commercially available galvanostatic pulse device was used (GalvaPulse™). The device has an Ag/AgCl reference electrode and concentrically placed annular counter and guard-ring zinc electrodes with outer/inner diameters of 60/30 and 100/80 mm, respectively. A galvanostatic current of 25 or 100 μA was applied to measure corrosion rates of passive or actively corroding steel, respectively. For all cases, the measurement time used was 10 s and the measurement was taken at the middle of the reinforcement. The guard-ring current was controlled automatically by the device to maintain the initial potential differences between the counter electrode and the reinforcement as well as the guard-ring electrode and the reinforcement. In this setup, the polarized length of rebar is assumed to be 70 mm.

The potentiodynamic technique relies on sweeping the electrode potential of rebar in a narrow range of its open circuit potential and measuring the response current. When the potential sweep range is kept small (e.g., ± 10 mV), the relationship between the potential change and response current would be linear with a slope that is equal to the sum of the polarization resistance (R_p) and the ohmic resistance (R) of the corroding system. Therefore, polarization resistance can be determined by subtracting the ohmic resistance from

the slope of the potential-current response line. A commercial potentiostat/frequency response analyzer (Gamry Reference 600™) was used for all potentiodynamic measurements. A 120 mm long, 60 mm wide, 5 mm high stainless-steel plate was used as a counter electrode mounted on the concrete surface at the middle of the rebar area. The potential was recorded through an Ag/AgCl electrode that was fixed in a hole in the middle of the counter electrode. The potential was swept from -10 to $+10$ mV with respect to the open-circuit potential with a potential scan rate of 0.167 mV/s as per ASTM G59,^[38] and the resulting current was measured. The ohmic resistance (R_Ω) was obtained using EIS through the impedance coinciding with the minimum negative phase shift. Although no confinement technique was used in this measurement, it was assumed that the area under the counter electrode is the polarized area (area corresponding to 120 mm of rebar length) since the scan range of electrode potential and the response current were small compared to the galvanostatic technique.

The coulometric technique relies on obtaining the polarization resistance through analyzing the potential transient obtained after the application of a certain, predefined, amount of electrical charge. The polarization resistance is obtained through fitting the experimentally obtained potential response to the theoretical one obtained due to the application of a quantity of charge to the Randles circuit.^[36,37,39,40] In this study, a commercial device was used (The Coulostat™) which had a circular stainless-steel electrode of 60 mm in diameter with an Ag/AgCl electrode at the center of the counter electrode. A current of 4 mA was applied for 50 ms resulting in a total applied charge of 200 mC. The response potential was collected for 30 s. The polarized area was assumed to be the full rebar specimen (area corresponding to 250 mm of rebar length) due to the device applying a current with a relatively high magnitude and the absence of a current confinement technique.

In EIS, a sinusoidal AC voltage is applied in a wide range of frequencies, and the impedance characteristics of the system (real and imaginary impedance as well as phase angle) are recorded through analyzing the applied voltage shift and the corresponding current for each frequency. The analysis procedure typically used in the literature for finding the polarization resistance is through fitting the resulting impedance spectra to that of an equivalent circuit that is assumed to represent the analyzed system.^[7,10–13,41] A simplified alternative approach includes the subtraction of high frequency impedance, representing ohmic resistance (R_Ω) of concrete, from the low frequency impedance, representing the sum of concrete resistance and polarization resistance ($R_p + R$). In this study, the second approach is used in order to eliminate the effect of the equivalent circuit model choice on the polarization resistance estimation. For this purpose, a commercial potentiostat/frequency response

analyzer was used (Gamry Reference 600™) to perform EIS using the same counter electrode setup that is described for the potentiodynamic technique. The amplitude of the applied AC potential from the open-circuit potential was in the range of ± 10 to ± 30 mV, depending on the cover depth and concrete resistivity. The EIS measurements were done between 100 kHz to 0.001 Hz. It was assumed that the area under the counter electrode is the polarized area (area corresponding to 120 mm of rebar length).

The CEPRA technique relies on using a four-probe Wenner-array setup and analyzing the potential response (i.e., voltage difference between the two inner probes) to a narrow DC current applied from the outer probes for a short period of time (6–10 s). Unlike other techniques, the CEPRA technique does not require a direct connection to the reinforcement. In order to find the polarization resistance, the potential response is fitted to a circuit model representing the steel-concrete system, as outlined in refs. [29–31]. In this study, a commercial device was used (iCOR™) which implements a four-point array with an electrode spacing of 50 mm; with the surface-mounted array being parallel to the rebar. The outer probes were used to apply a narrow DC step current for 6 s, and the voltage difference between the two inner probes was recorded with a sampling rate of 3 Hz. The details of corrosion rate calculation from the obtained potential response is outlined by Fahim et al.^[30]

Table 1 provides the comparison of critical features of different corrosion rate measurement techniques that are studied in this paper.

2.3 | Experimental procedure

Weekly corrosion rate measurements were conducted on all slabs using the galvanostatic pulse technique, potentiodynamic polarization technique, coulometric technique, and CEPRA technique for a period of 7 months. Due to the long duration required by EIS measurements, only two measurements were taken between 3 and 4 months of exposure when it was found that the corrosion rates stabilized. After 7 months, the specimens were removed from the containers and left

to dry in laboratory conditions ($T = 20\text{--}25$ °C and $RH = 30\text{--}70\%$) for a month during which corrosion rate measurements were conducted weekly in order to analyze the effect of the increased resistivity on the results.

At the end of the exposure period (a total of 8 months), rebars were extracted by inducing a longitudinal crack along the reinforcement using a jackhammer. Top and bottom sides of the rebars were photographed to show the extent of corrosion and to allow for the calculation of the corroded area to total area ratio (termed C/T herein). The mass loss of the reinforcements was done according to the ASTM G1^[32] procedure C.3.5, and the average corrosion rates were calculated from the mass loss results calculated according to Faraday's law.

The digital images of the rebar specimens were analyzed using imageJ software^[42] to determine the corroded area to total area ratio (C/T). This was done to yield empirical observations on the role of the percent of corroded area on the accuracy of these techniques as shown later. This procedure was done by manual color threshold adjustment on photographs of the rebar specimens in order to differentiate between three primary features: (1) the corroded areas; (2) the mortar adhering to the rebar surface; and (3) the non-corroded steel surface.

3 | RESULTS AND DISCUSSION

This section compares the average corrosion rates obtained from the existing methods typically used for reinforced concrete elements and average corrosion rates obtained using gravimetric (mass loss) measurements following the ASTM G01^[32] procedure. This section also critically analyzes the reasons for the observed differences and highlights ways to enhance the accuracy of the techniques. Since the corrosion measurement techniques used in this study provide instantaneous corrosion rates, and gravimetric approach provides average corrosion rates, the average electrochemically determined corrosion rate was obtained by integrating the corrosion rates obtained by the technique throughout the monitoring period (8 months) divided by the total period of exposure.

TABLE 1 Comparison of critical features of different corrosion rate measurement techniques

	GP	PD	CS	EIS	CEPRA
AC/DC	DC	DC	DC	AC	DC
Applied potential/current	25–100 μ A	–10 to 10 mV	200 mC	10–30 mV	500–2000 μ A
Assumed polarized length (mm)	70	120	250	120	250
Connection to rebar	Yes	Yes	Yes	Yes	No
Uses guard ring	Yes	No	No	No	No
Measurement duration (s)	10	≈ 120	30	10,800–18,000	6

3.1 | Galvanostatic pulse technique

Figure 2 presents the average corrosion rate determined by the galvanostatic technique plotted versus the average corrosion rate obtained using the mass loss data.

The results clearly show an overestimation of corrosion rates ($\sim 1 \mu\text{A}/\text{cm}^2$) given by the galvanostatic pulse technique for blocks without admixed chlorides; that is, passive reinforcements. This overestimation is in agreement with reported data from the literature^[9,14,15,19,43–45] and is believed to be the result of several assumptions used by the device used. The galvanostatic pulse device uses a similar current confinement procedure for both active and passive corrosion states, which is an assumption that has been shown to be inaccurate due to the high resistance to polarization exhibited by passive steel.^[9,43,45] For passive reinforcements, it has been shown^[9,45,46] that the high polarization resistance and the high anodic Tafel coefficient (due to passivation control) cause the applied currents from the counter electrode and guard ring to propagate laterally, and distribute throughout the reinforcement surface, to areas away from the counter electrode; yielding the assumed polarized area smaller than the actual one. Furthermore, the additional current from the guard ring is not considered in corrosion rate calculations; therefore, it is another source of error for passive steel.^[44] The third reason for the overestimation of corrosion rates for passive reinforcement, and perhaps the most significant one, is the short measurement duration used. The measurement time for the device that was used in this study was 10 s, which is considerably smaller than the time required for passive electrodes to reach quasi-steady-state conditions, under the current applied by the device ($25 \mu\text{A}$), as shown by Martinez et al.^[19] This leads to an underestimation of R_p , and further contributes to the overestimation of i_{corr} , along with the other sources of errors.

The estimated average corrosion rates for the blocks with admixed chlorides (actively corroding specimens) agree well with actual average corrosion rates, with the ratio between the predicted and actual corrosion rates being in the range of 0.5 to 2 for most of the specimens, which is the typically accepted range in the literature.^[47] This range is based on the uncertainty range for Tafel coefficients; which have been shown to range from 13 to 52 mV. A review of the relevant literature^[9,16,43,45,48] reveals that several factors affect the flow of the polarizing current, which also influences the polarized area and corrosion rates. Such factors include concrete resistivity and cover depth^[16,43,45,48], as well as corroded area to total area ratio (C/T).^[9] In general, the lateral flow of current along the reinforcement to polarize areas away from the counter electrode increases with decreasing concrete resistivity, as shown in refs. [16,43,45], increasing cover thickness, as shown in refs. [16,45,48], or decreasing C/T in the vicinity of the counter electrode area.^[9,46] This causes an overestimation of the current flowing under the counter electrode. However, as shown in Figure 2, the individual effects of these factors on the difference between estimated and actual corrosion rates are not clear. The combined effect of these factors is demonstrated in Figure 3, which shows the change of the ratio between estimated (using galvanostatic pulse technique) and actual average corrosion rates as a function of an aggregated term that includes the admixed chloride content (Cl%), cover depth, ohmic resistance (R_Ω) and the corroded-to-total area ratio (C/T) obtained from image analysis.

Figure 3 shows a good correlation between this aggregated term and the ratio between estimated and actual corrosion rates. This relationship indicates that as the ohmic resistance decreases, or as the chloride content increases, an overestimation of corrosion rates occurs.

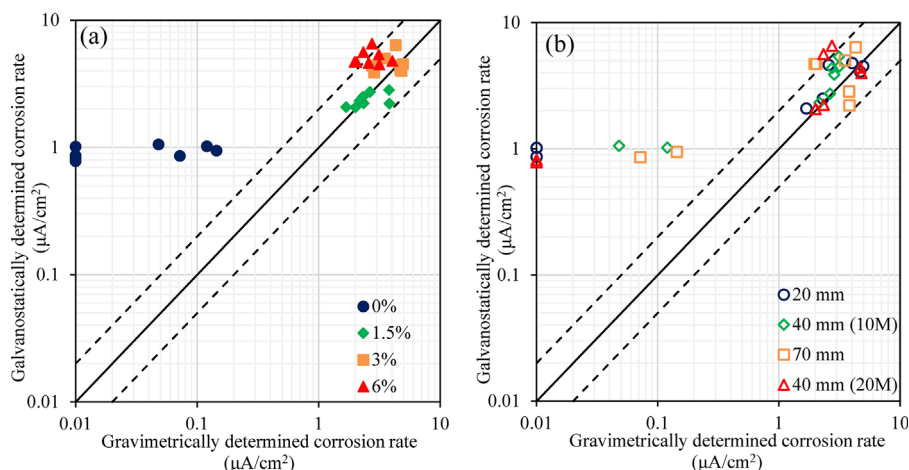


FIGURE 2 Results obtained from the galvanostatic pulse technique compared to the gravimetrically obtained corrosion rates: (a) as a factor of admixed chloride percentage and (b) as a factor of cover depth and reinforcement diameter [Color figure can be viewed at wileyonlinelibrary.com]

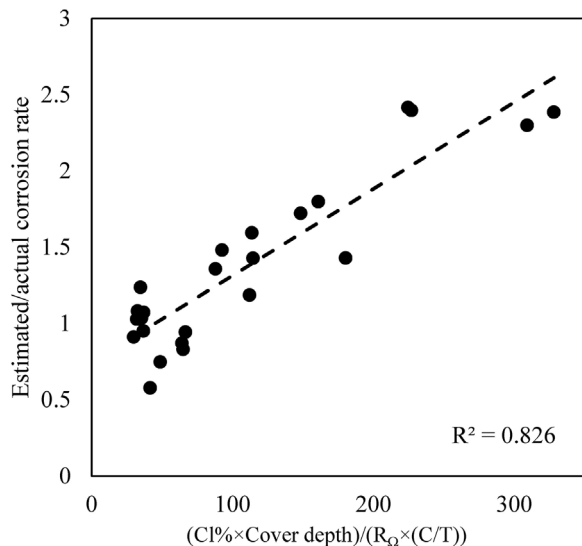


FIGURE 3 The mixed effect of steel/concrete characteristics on the accuracy of the galvanostatic technique

Both processes are associated with decrease in the electrical resistivity of concrete, which increases lateral current flow (both from the counter electrode and the guard ring) and polarizes rebar surfaces away from the counter electrode. This lateral flow leads to less current flowing to the rebar area under consideration (the polarized area) than that assumed by the device, which leads to an overestimation of the corrosion rate. This may also be partially attributed to the decreased resistivity causing an increased influence of macrocell corrosion, on the expense of microcell corrosion, which leads to a decrease in the applicability of Stern and Geary's equation. Figure 3 also implies that the difference between the estimated and actual average corrosion rates increases with increasing cover thickness. For large cover depths, the current has higher tendency to laterally propagate within concrete cover and polarizes areas away from the counter electrode, which leads to the underestimation of the polarizing current of the rebar under the counter electrode and overestimation of the corrosion rate, as also shown in refs. [16,48]. Finally, it can be seen in Figure 3 that increasing corroding area (C/T) corresponds to a decrease in the difference between measured and actual corrosion rates. It is hypothesized that if C/T is high, there is a high availability of anodes that can consume the applied current near the counter electrode^[9] and decrease its tendency to disperse to areas far from the counter electrode, hence reducing the difference between the assumed and actual polarizing current reaching the area under the counter electrode. This may also be attributed to the larger contribution of microcell corrosion, for rebars with larger observed corroded areas, to the measured corrosion rate, on the expense of macrocell corrosion.

3.2 | Potentiodynamic technique

Figure 4 presents the average corrosion rate determined by the potentiodynamic technique plotted versus the average corrosion rate obtained using the mass loss data.

The potentiodynamic technique results showed a better estimation of the passive corrosion rates than those obtained using the galvanostatic pulse technique. All corrosion rates for passive reinforcements were in the range of $0.3\text{--}0.5\ \mu\text{A}/\text{cm}^2$. Although this allows differentiating passive and active reinforcements, these measurements are still higher than the typical range used for detecting passivity in the civil engineering literature (less than $0.1\ \mu\text{A}/\text{cm}^2$). This is mainly due to the fast scan rates used for practical reasons so that the technique can be used in the field in a reasonable measurement timeframe.^[49,50] Slower scan rates (e.g., $0.05\ \text{mV}/\text{s}$), which are less practical for field applications, were tried and were found to yield passive corrosion rates in the range of $0.1\text{--}0.3\ \mu\text{A}/\text{cm}^2$, which are closer to the typically accepted passive corrosion rates.

For the actively corroding reinforcements, the estimated corrosion rates agreed well with the gravimetrically obtained data, with the ratio between predicted and actual corrosion rates generally falling in the range accepted in the literature. This is remarkable considering that the technique does not use a current confinement technique and the assumed polarized area is the one under the counter electrode. The same empirical function that was developed for the galvanostatic technique seemed to apply for the potentiodynamic technique, as shown in Figure 5, with the addition of the polarization resistance value to the denominator of the mixed factors term. This term was added because the current applied from the counter electrode is dependent on polarization resistance. The strength of this correlation for both cases of galvanostatic and potentiodynamic techniques clearly questions the concept of “constant polarized area” and shows that the assumption of a specific polarized area for any concrete resistivity or cover depth is an approach that may yield misleading results. This issue is further exacerbated by the availability of galvanic corrosion and the randomness of anode locations with respect to the counter electrode.^[9] Nevertheless, results by this study still show that adequate results can be provided by these techniques, in laboratory setups, when using a constant polarized area. The hypotheses outlined in Figures 3 and 5, on the effect of resistivity, cover depth and C/T on the errors in corrosion rate measurements, will be investigated further in a subsequent paper from theoretical and numerical points of views.

Figure 6 shows the corrosion rate results obtained by the potentiodynamic technique before correction for the IR-drop. As expected, the corrosion rates are generally underestimated in cases for which the ohmic resistance is not corrected. However, ignoring the ohmic resistance did not produce

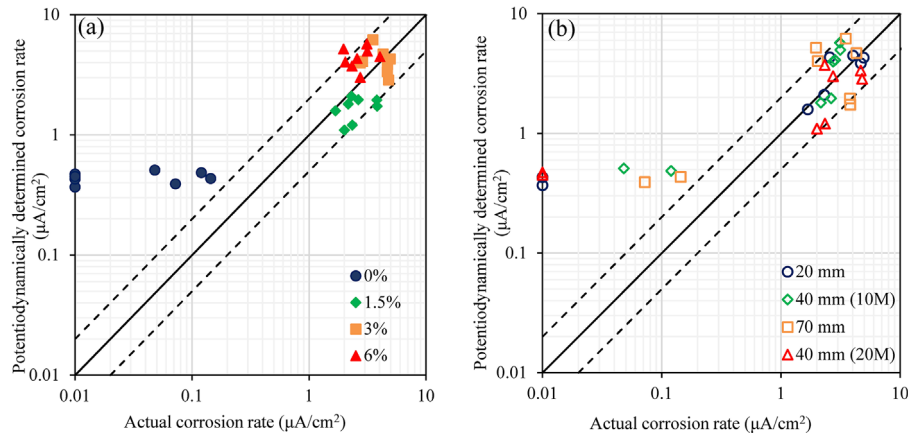


FIGURE 4 Results obtained from the potentiodynamic technique compared to the gravimetrically obtained corrosion rates: (a) as a factor of admixed chloride percentage and (b) as a factor of cover depth and reinforcement diameter [Color figure can be viewed at [wileyonlinelibrary.com](#)]

significant errors for concrete with saturated low resistivity concrete as those used in this study (resistivities were in the range of 15–200 ohm m for these specimens). The ohmic drop (R_{Ω}) was found to be in the range of 12 and 30% of polarization resistance (R_p) for the passive and active conditions, respectively. In the dry condition, however, R_{Ω} was found, in many cases, to be higher than R_p (specifically for cases with cover depths of 70 mm). In these cases, ohmic resistance compensation would be essential in predicting corrosion rates accurately. It should be noted that the ohmic resistance correction used for this study was obtained from EIS through determining the total impedance coinciding with the minimum negative phase shift observed at high frequencies. Such a measurement only takes a few seconds

and shows a good advancement in the determination of corrosion rates. This was chosen over the typically used current-interruption method due to severe distortions of polarization curves observed when using this method. The issues with current-interruption methods in cases with low conductivity media and low time constants are well-documented and can be found in refs. [20,21,51,52].

3.3 | Coulostatic technique

Figure 7 presents the average corrosion rate determined by the coulostatic technique plotted versus the average corrosion rate obtained using the mass-loss data.

The results demonstrate the ability of the technique in determining the passive corrosion rates. The corrosion rates obtained for the specimen with no admixed chlorides was

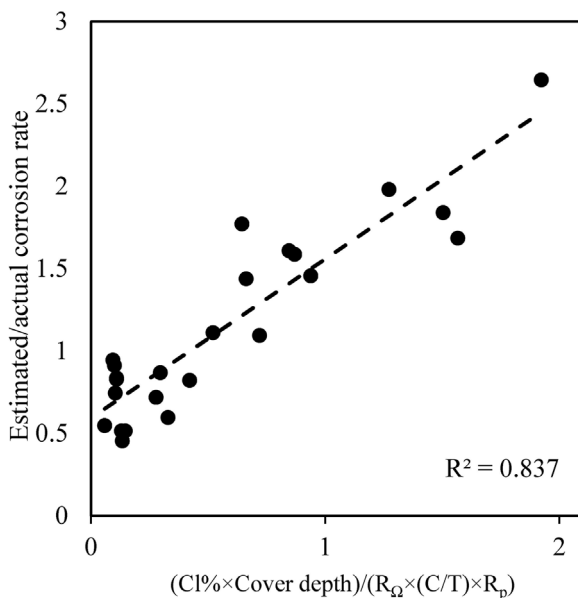


FIGURE 5 The mixed effect of steel/concrete characteristics on the accuracy of the potentiodynamic technique

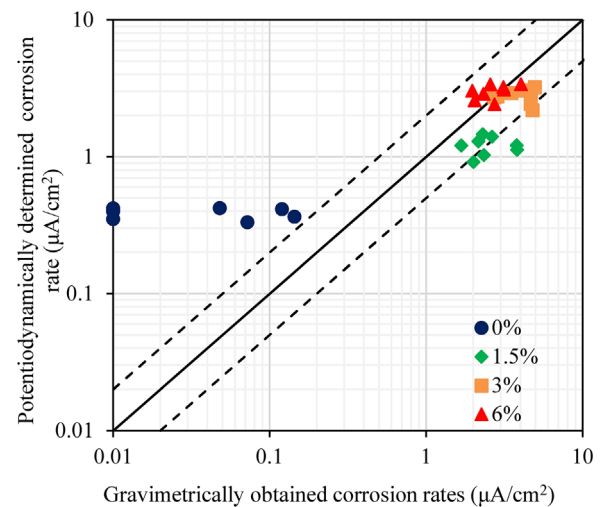


FIGURE 6 Corrosion rates obtained with the potentiodynamic technique without ohmic resistance correction [Color figure can be viewed at [wileyonlinelibrary.com](#)]

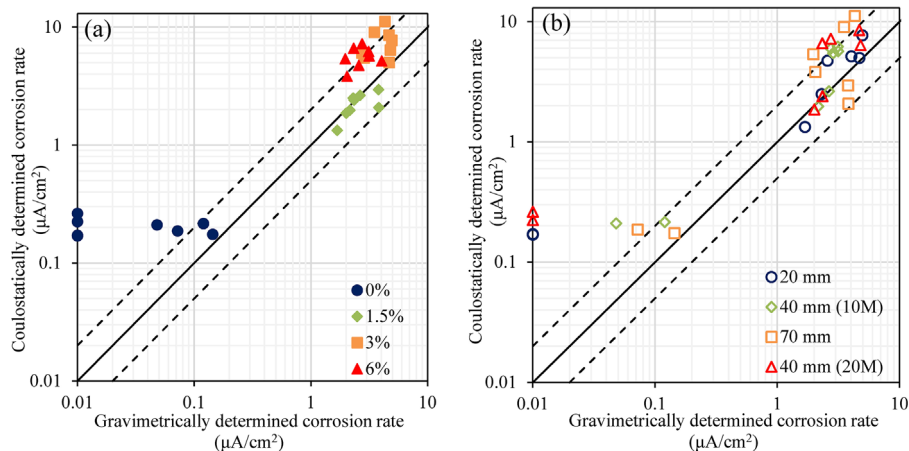


FIGURE 7 Results obtained from the coulometric technique compared to the gravimetrically obtained corrosion rates: (a) as a factor of admixed chloride percentage and (b) as a factor of cover depth and reinforcement diameter [Color figure can be viewed at wileyonlinelibrary.com]

around $0.2 \mu\text{A}/\text{cm}^2$. However, it should be noted that the device used for the coulometric technique does not use current confinement and applies a constant amount of charge regardless of the corrosion state of rebar in concrete. As a result, it was assumed that the full reinforcement area is polarized; therefore, the success in determining passive corrosion rates is mainly due to this assumption, which limits the applicability of the used device to laboratory studies and small specimens for which the polarized area is relatively confined and known.

In general, the coulometric technique provided accurate estimates of corrosion rates for actively corroding reinforcements; however, corrosion rates of some of the specimens with high chloride contamination were overestimated, as shown in Figure 7. This overestimation is in line with results reported in the literature.^[36,37,40]

The coulometric method relies on the assumption that the response of a metal/electrolyte system to an electrical signal is similar to that of an equivalent Randles circuit. Therefore, when a known amount of charge is applied, the observed instantaneous potential response, η_o , is assumed to be a function of only the double-layer capacitance, C_{dl} , on the rebar surface. The rebar surface is then assumed to discharge the applied charge over a period toward the original corrosion potential. The potential of the rebar at a given time after the initial current application can be written as:

$$\eta_t = \eta_o \exp\left(\frac{-t}{\tau_c}\right) \quad (2)$$

where η_t (mV) is the potential shift at any time t (s), η_o (mV) is the initial potential shift, and τ_c (s) is the coulometric time constant ($C_{dl}R_p$).

The above equation does not contain any term for the electrolyte resistance or electrolyte capacitance because the

assumed Randles circuit implies that the electrolyte behaves in a purely resistive manner with no associated capacitive behavior. This means that the electrolyte cannot be charged; therefore, the response is not dependent on the electrolyte properties.^[36,40] However, as shown in Figure 8, this is not strictly correct. After the charge is applied, the potential shift includes two observed time constants, as shown in Figure 8a. The first one is due to the capacitive nature of the concrete, as shown in refs. [36,39,40] and supported by EIS results shown in section 3.5, and the second one is due to the capacitive nature of the electrode surface. The Randles circuit assumption does not allow for the inclusion of the first time constant, hence, may lead to substantial errors. EIS results by the current study and a number of other authors^[7,12,13,53,54] clearly indicate that concrete exhibits a capacitive behavior, albeit orders of magnitude smaller than that associated with the double-layer capacitance of rebar surface. Since the equation used to determine the polarization resistance only takes into consideration the capacitive behavior of the electrode and not the electrolyte, the method used to obtain the polarization resistance was to remove the first second out of the transient, in which the electrolytic capacitive forces are assumed to be exhausted and the electrolyte capacitance fully discharges. The remaining part is then fitted to the previously shown Randles circuit response (Eq. 2). This is illustrated schematically in Figure 8b.

For all of the cases, the fitted curve, after the removal of the first second of the observed response, was similar to that shown in Figure 8c. It is clear that the fitted curve underestimates the initial potential shift. This is due, in part, to the difficulty in dividing the potential relaxation to distinct regions of electrolyte contribution and interface contribution. Therefore, when the first second is removed, some of the early response from the double-layer time constant are removed, wrongly, in the excluded part.

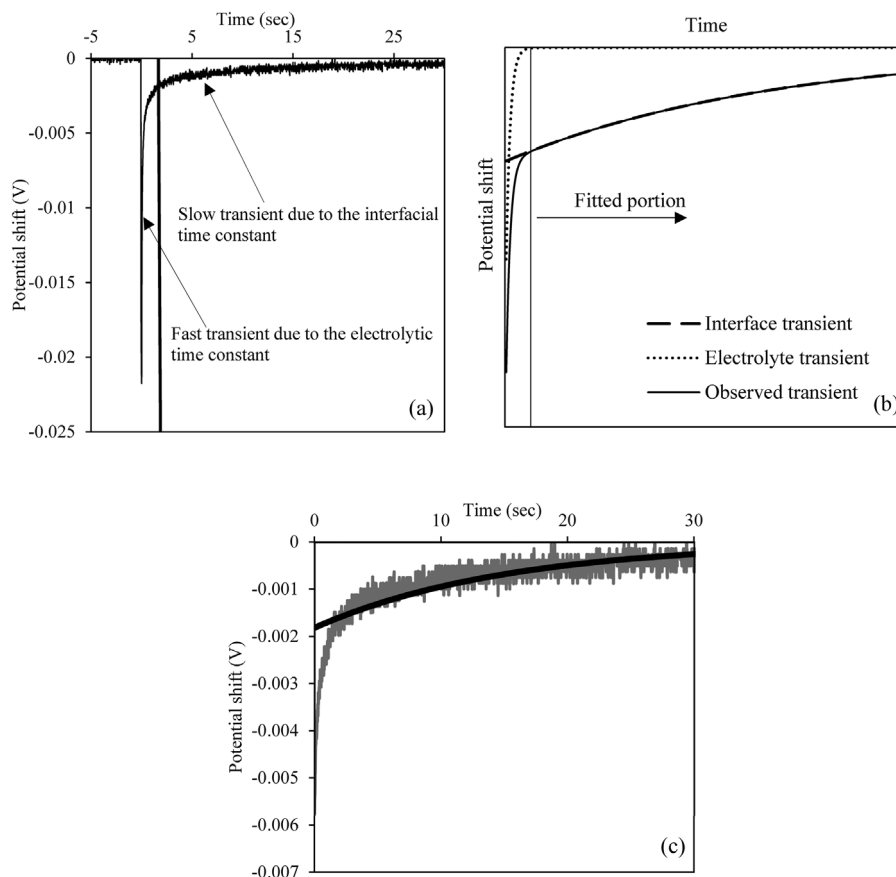


FIGURE 8 (a) Typical experimentally obtained potential transient, (b) a schematic of the method used to fit the experimental transient, (c) experimentally obtained transient (after removal of the first second of data) compared to that fitted through Eq. (2)

Furthermore, a higher final potential shift is determined when fitting Eq. (2) to the data as shown in Figure 8c. This may indicate that the very fast or very slow regions of the interfacial transient did not contribute to the polarization resistance which agrees with results by Hassanein et al.^[40]

In order to further demonstrate the aforementioned issue with fitting the transient to the theoretical Randles circuit response, Laplace transformation was performed on the obtained potential transients in order to obtain Nyquist plots of imaginary versus real impedance, using the procedure described by Pilla.^[55] A typical Nyquist plot of a coulometric measurement is shown in Figure 9. The loops in the high frequency region (portion of the spectrum in which the real impedance is less than 50 ohms) may indicate simultaneous charging and discharging of the electrolyte capacitance. Although not shown in Figure 9 for clarity, this behavior was seen in all cases. Furthermore, it is rather clear that the transient associated with the electrolyte time constant overlaps with that associated with the interfacial time constant, which introduces complications in the separation of these time constants in the manner shown previously. The continuous charging and discharging behavior of the electrolyte capacitance may indicate that the behavior

assumed in fitting the experimental results, which is shown in Figure 8b, does not exist and may lead to serious errors. In simple terms, the electrolyte capacitance may not behave as that shown in Figure 8b (one discharging time transient) but as several consecutive charging and discharging transients which cannot be removed as in the procedure used.

Glass^[36] also hypothesized about a similar behavior and noted that the shape of the transient may be affected by the

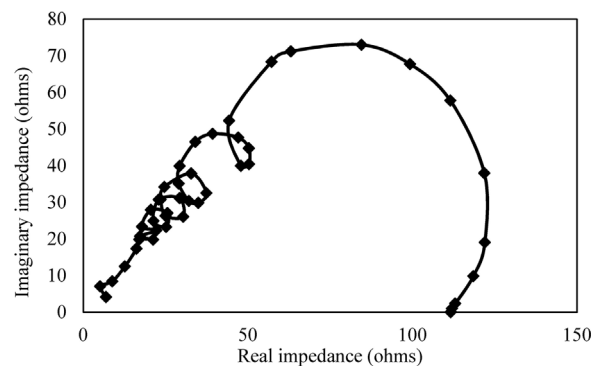


FIGURE 9 Example of the real vs. imaginary impedance of the obtained response

charging period when some discharge of the associated capacitance occurs simultaneously during charging which in turn will lead to a reduction in the measured potential shift. The author demonstrated that this is more sensitive to errors resulting from the residual effects of faster transients. Furthermore, results by Hassanein et al.^[40] demonstrated that it is unlikely for the coulometrically obtained transient to produce average values of these parameters if deviations from an exponential transient behavior occur. Such deviations may result when measuring dispersed time constants (produced by a position-dependent electrolyte resistance, polarization resistance, and interfacial capacitance). The impedance spectrum obtained from the actual transient would be, in these cases, determined by the minimum electrolyte resistance at very high frequencies and the combination of all resistances at very low frequencies,^[40] which can also explain the overestimation of corrosion rates obtained.

Although there are errors in the fitting procedure, the results shown in Figure 7 indicate that practically acceptable corrosion rate measurements can still be obtained using the coulometric method; provided that the polarized area is known. In order to more accurately estimate corrosion rates, the capacitance of the electrolyte has to be put into consideration. This can be done through a Laplace transformation procedure such as that shown in this study. Results by Christodoulou et al.^[56] demonstrate the feasibility of the approach of determining corrosion rate results from the Laplace transformation of obtained potential transients.

3.4 | CEPRA technique

Figure 10 presents the average corrosion rate determined by the CEPRA technique plotted versus the average corrosion rate obtained using the mass loss data. The average of corrosion rate measurements taken during the drying period for passive reinforcements is also included in Figure 10 since saturation was found to affect the measured corrosion rates for this technique significantly, compared to other techniques.

For the actively corroding specimens, the predicted corrosion rates agreed well with the actual corrosion rates. Results for 21 out of 24 specimens fell in the range of results typically accepted in the literature. The remaining three specimens showed corrosion rates that were 35–45% of the actual corrosion rate. This underestimation was found for specimens with 1.5% admixed chlorides for both 20 M reinforcement diameter and for one 20 mm cover depth specimen with 3% admixed chlorides. This may be primarily attributed to errors associated with polarized area assumption. In these cases, it was assumed that the full reinforcement area is the polarized area. However, as noted earlier, the polarized area changes dramatically due to changes in several factors. In the case of 1.5% chloride (highest resistivity of all active specimens), or in cases of low cover depths (20 mm), the

assumption of polarization of the full reinforcement may not be correct. In the case of 20 M reinforcement, there is a much higher circumferential area that can drain the polarizing current (compared to other 10 M reinforcements) which also does not allow the current to disperse and polarize the whole area.

For the specimens without admixed chlorides, the results showed an overestimation of corrosion rates for the case of saturated specimens with 10 M reinforcement for which the results fall in the range of 0.6–0.8 $\mu\text{A}/\text{cm}^2$. This, however, was not the case for the passive 20 M specimens in which corrosion rates in the range of 0.2 $\mu\text{A}/\text{cm}^2$ were found. When the passive specimens were tested during the drying period, the measured corrosion rates were lower than 0.25 $\mu\text{A}/\text{cm}^2$. In the semi-saturated conditions (after 1 day of drying), the results were in the range of 0.4 $\mu\text{A}/\text{cm}^2$; which represents cases of semi-saturated concrete that better resemble field cases.

The primary reason for the overestimation noted for the passive cases in saturated conditions with small rebar diameters is that the CEPRA model assumes that the high-frequency (after a few milliseconds from the application of the polarizing current) and low-frequency (at steady-state) current flow paths are similar, but one is governed by the double-layer capacitance and another is governed by the polarization resistance. The similarity between the two paths is essential for applying the model and obtaining acceptable results. Finite element modeling results in refs. [25,30,31] indicate that the high- and low-frequency paths are rather similar in cases of actively corroding electrodes. However, this is not the case for passive reinforcements because the reinforcement's double-layer acts as a relatively good current-consumer (causing a short-circuit effect) in the high frequency portion, while in the low frequency region, passive reinforcements act as a current insulator (due to the high polarization resistance) and hardly any current polarizes the rebar. Therefore, in the high frequency ranges, most of the current charges the double-layer capacitance instead of flowing between the two polarizing probes, while in the low frequency ranges, most of the current flows in the concrete cover between the polarizing probes. The low- and high-frequency current paths will tend to become more similar when the current flowing to the reinforcement (as opposed to that flowing in the concrete cover between the two outer probes) in the low-frequency range increases. This current increases as the electrode's area available for current consumption increases or as the system resistivity increases; which explains the good results obtained for the 20 M reinforcements and for the dry or semi-saturated (high resistivity) cases.

The effect of the measurement time is also a crucial factor. The CEPRA device relies on analyzing the response of the electrode, for 6–10 s, to an applied pulse. As noted

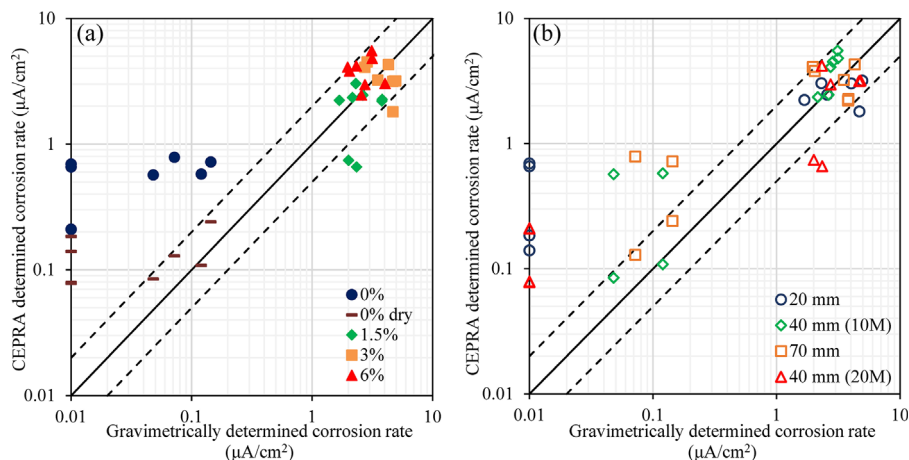


FIGURE 10 Results obtained from the CEPR technique compared to the gravimetrically obtained corrosion rates: (a) as a factor of admixed chloride percentage and (b) as a factor of cover depth and reinforcement diameter [Color figure can be viewed at wileyonlinelibrary.com]

earlier in the galvanostatic technique, the time constant associated with passive reinforcements is factors of much higher than that for the active cases. If the electrode requires more than 6 s to reach quasi-steady-state conditions, the potential shift will be underestimated which may cause some errors. Modeling has, however, shown that this method highly decreases the time required for measurements.^[30,31] This is in agreement with experimental results by Lim et al.^[57] and Zhang et al.^[22] This is due to the very low currents reaching the electrode compared to the galvanostatic technique. It should be noted, in any case, that comparing the results obtained for saturated versus dry conditions shows evidence that the effect of the measurement time is a secondary factor compared to the effect of the system's resistivity or the electrode's area.

In summary, the applicability of this method and its accuracy is clearly shown from the results of this study for laboratory cases. The overestimation of passive corrosion rates for the saturated specimens with small reinforcement diameters is expected in the range of very low resistivity

concrete used in this study. Such an overestimation is very similar to that for conventionally used techniques (such as the galvanostatic pulse method). The good correlations obtained between the electrochemically predicted and actual corrosion rates for the case of actively corroding reinforcements is very similar to those shown for the other well-established techniques. This accuracy was not only attained without a reinforcement connection, but also in a measurement time of only 6 s which is much shorter than the measurement durations used for other techniques.

3.5 | EIS technique

Figure 11 presents the average corrosion rate determined by the EIS technique plotted versus the actual corrosion rate obtained using the mass loss data.

EIS provided accurate results in both passive and active states. As noted earlier, the polarization resistance was obtained without using any circuit modeling, but by determining the difference between the high- and low-frequency

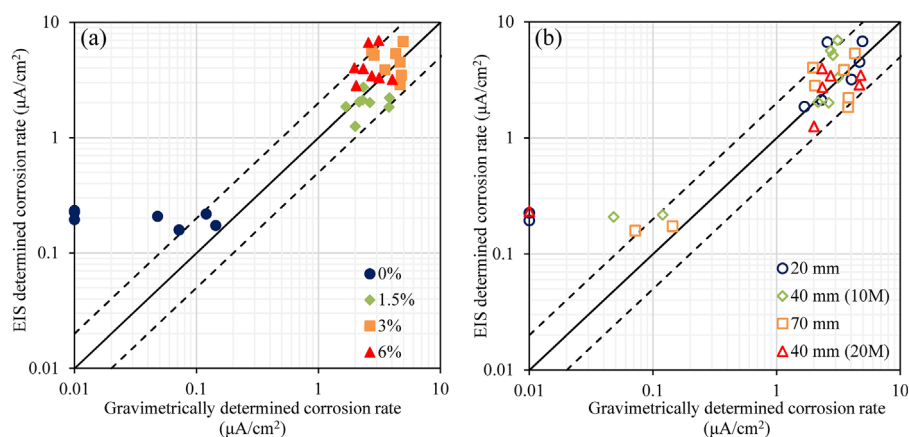


FIGURE 11 Results obtained from the EIS technique compared to the gravimetrically obtained corrosion rates: (a) as a factor of admixed chloride percentage and (b) as a factor of cover depth and reinforcement diameter [Color figure can be viewed at wileyonlinelibrary.com]

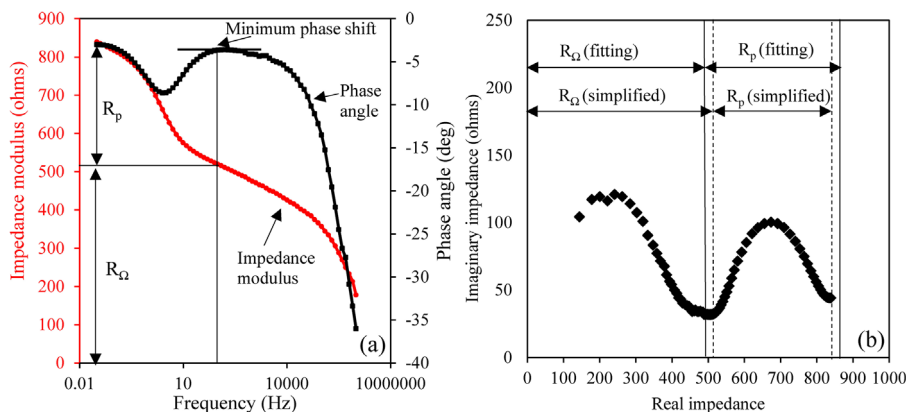


FIGURE 12 (a) Bode plot obtained for an actively corroding specimen and (b) Nyquist plot obtained for an actively corroding specimen [Color figure can be viewed at wileyonlinelibrary.com]

impedance responses. For several cases, the total impedance was not a constant in the very high frequencies. In these cases, the ohmic resistance was obtained as the total impedance coinciding with the minimum negative phase shift obtained in the high-frequency region.^[18] The polarization resistance was then obtained as the difference between the low frequency total impedance subtracted by the ohmic resistance. This procedure is illustrated schematically in Figure 12a. The results obtained through this procedure, compared to those obtained from curve fitting using the circuit proposed by Christensen et al.,^[13] which was found to fit the obtained transient satisfactorily, can be seen through the vertical lines in the Nyquist plot shown in Figure 12b. The fitted and simplified procedures yield similar results; because the imaginary impedance diminishes in the very low frequency range and the total impedance, obtained from the Bode plot, can be approximated to the real impedance (note that the imaginary impedance is only 44 ohms while the real impedance is 838 ohms in the very low frequencies which leads to an impedance modulus of 840).

The passive corrosion rate results showed a good estimate of corrosion rates, when the aforementioned procedure was used, with all corrosion rates falling in the range of $0.2 \mu\text{A}/\text{cm}^2$. Although these results are in the range of accepted results for passivity detection, better estimates could have been achieved if the EIS scans were performed at lower frequencies than 0.001 Hz. However, this would require significantly longer measurement times.

Figure 13 shows the Bode and Nyquist plots obtained for one of the passive specimens. The ohmic resistance estimated from the simplified procedure coincides well with that estimated by curve fitting, using the circuit in Christensen et al.^[13] However, when curve fitting was performed using the circuit model in Christensen et al.,^[13] the polarization resistance was more than four times that shown by the simplified approach. It should be noted that for passive reinforcements, the low frequency impedance modulus contains a contribution from both the real and imaginary impedance. As shown in Figure 13, the low-frequency impedance response did not reach a plateau (the

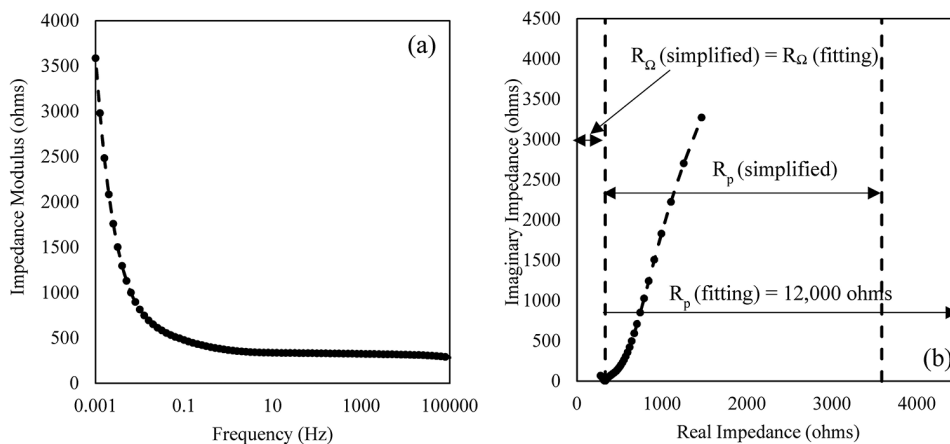


FIGURE 13 (a) Bode plot obtained for a passive specimen and (b) Nyquist plot obtained for a passive specimen

imaginary impedance did not reach negligible values). This means that frequencies as low as 0.001 Hz are not low enough to mitigate the capacitance effect caused by the double-layer capacitance. Using this low-frequency impedance modulus as the real impedance in the Nyquist plot is a crude approximation (very different from the case shown in Figure 12 where the imaginary impedance diminishes). If a lower frequency response is used, then a better estimate of the passive corrosion range would be found. However, reaching frequencies lower than 0.001 Hz is not a feasible option for field assessment since achieving one measurement at such low frequencies requires hours of potential sweeping. In these cases, it was found that fitting the full experimental results (Nyquist plots) to a certain circuit model would yield better results for which the corrosion rates are less than $0.05 \mu\text{A}/\text{cm}^2$. However, this demands a full set of data with impedance responses from a wide range of frequencies and a substantial understanding of the electrochemical meaning of the circuit models used. This shows that, although the use of circuit models is very valuable in identifying the electrochemical cell components, it is not essential in differentiating passive and active reinforcements. This simplified approach is not recommended for research applications in which EIS is typically used to collect substantial information about the system's characteristics, and a high-precision estimation of the corrosion rate is required. However, for practical applications among the civil engineering community, in which an electrochemical understanding of techniques such as EIS is not common practice, such an approach can be used to obtain a rough estimate of the corrosion rate in a much-shortened analysis time.

It should be noted that 1/8 of the exposure period the specimens were in dry condition which may explain why EIS overestimated some of the corrosion rates since EIS measurements was taken in the saturated condition and extrapolated for the full exposure period. Again, the same overestimation of corrosion rate in the 6% reinforcements can be seen with EIS. This is believed to be attributed to the polarized area reaching higher values than those assumed by the technique in such low resistivity system as discussed earlier.

4 | CONCLUSIONS

The following conclusions can be drawn based on the presented results:

- The galvanostatic technique failed in detecting passivity. However, the technique provided accurate results for the actively corroding reinforcements.
- The potentiodynamic technique provided an acceptable passive corrosion rate determination without the need for a current confinement technique. However, the estimation of passive corrosion rates could be enhanced using slower scan rates. The technique also showed accurate corrosion rate results for actively corroding reinforcements.
- The coulometric technique provided the lowest corrosion rates of all the techniques studied for the passive case. However, this is mainly due to the polarized area being well-determined in laboratory conditions. The coulometric technique generally overestimated the active corrosion rates due to the Randles circuit not being able to capture the experimental transient. A method was suggested based on Laplace transformation of the obtained potential transients that can provide more accurate results.
- The CEPR technique provided accurate corrosion rate estimates for the actively corroding reinforcements. It also provided practically acceptable corrosion rates for passive conditions except for passive 10M reinforcements in saturated concrete; which was attributed to deviations from the assumed circuit model in these cases. The accuracy obtained through this method was not only obtained in a connectionless manner but also in a measurement time of only 6 s; which provides a substantial advantage over other well-established methods.
- EIS provided an accurate estimate of both the passive and active corrosion cases through a simplistic spectrum-analysis procedure; without the use of circuit models.
- All of the techniques generally overestimated the corrosion rate in the 6% admixed chloride specimens, which was hypothesized to be due the low system resistivity and the associated lateral dispersion of the polarizing current.
- The mixed effect of factors including cover depth, concrete resistivity, corroded-to-total area ratio and admixed chloride percentage was analyzed and was found to correlate well to the ratio of estimated/actual corrosion rates for potentiodynamic and galvanostatic techniques. This will be further investigated in a subsequent paper from theoretical and numerical viewpoints.

These conclusions clearly indicate that, for actively corroding reinforcements, the differences between the corrosion rates obtained by the techniques are rather minor. Any of these techniques could be used to capture corrosion rates for actively corroding reinforcements, with a practically acceptable accuracy, in cases where the reinforcement area is known (laboratory conditions). As outlined in this paper, there is evidence that this may not be the case for field conditions with ambiguous polarized area and random distribution of anodes. Further effort will be required in the future to evaluate the accuracy of these techniques in conditions with polarized area ambiguity. On the other hand, for passive reinforcements, it is clear that a

number of factors affect the accuracy, such as scan rates, measurement duration, applicability of circuit models, or confinement success. The effect of these parameters needs to be quantified in order to accurately detect passivity in the field.

ACKNOWLEDGMENTS

The authors would like to thank Dr. Allan Scott, from the University of Canterbury, for providing the device used to perform the coulometric measurements, as well as Dr. Edward Moffatt for his assistance during testing. MT and AF would also like to acknowledge the National Sciences and Engineering Research Council of Canada for the funding provided for this project.

ORCID

Andrew Fahim  <http://orcid.org/0000-0002-6210-2390>

REFERENCES

- [1] G. H. Koch, P. H. Brogers, N. Thompson, Y. P. Virmani, J. H. Payer, *Corrosion Cost and Preventive Strategies in the United States*, FHWA report; FHWA-RD-01-156, Federal Highway Administration, Washington, DC **2002**.
- [2] L. Bertolini, B. Elsener, P. Pedferri, E. Radaelli, R. Polder, *Corrosion of Steel in Concrete: Prevention, Diagnosis, Repair*. Wiley-VCH, Weinheim, Germany **2013**.
- [3] K. Sagoe-Crentsil, F. P. Glasser, *Mag. Conc. Res.* **1989**, *41*, 205.
- [4] F. M. Montemor, A. M. P. Simoes, M. G. S. Ferreira, *Corrosion* **1988**, *54*, 347.
- [5] P. Ghods, O. B. Isgor, G. McRae, T. Miller, *Cem. Conc. Comp.* **2009**, *31*, 2.
- [6] M. Stern, A. L. Geary, *J. Electrochem. Soc.* **1957**, *104*, 56.
- [7] I. Martínez, C. Andrade, *Mater. Corros.* **2011**, *62*, 932.
- [8] B. Elsener, *Corros. Sci.* **2005**, *47*, 3019.
- [9] P. V. Nygaard, M. R. Geiker, B. Elsener, *Mater. Struct.* **2009**, *42*, 1059.
- [10] D. G. John, P. C. Searson, J. L. Dawson, *Br. Corros. J.* **1981**, *16*, 102.
- [11] S. Feliu, J. A. González, C. Andrade, V. Feliu, *Mater. Struct.* **1989**, *22*, 199.
- [12] S. J. Ford, T. O. Mason, B. J. Christensen, R. T. Coverdale, H. M. Jennings, E. J. Garboczi, *J. Mater. Sci.* **1995**, *30*, 1217.
- [13] B. J. Christensen, T. Coverdale, R. A. Olson, S. J. Ford, E. J. Garboczi, H. M. Jennings, T. O. Mason, *J. Am. Ceram. Soc.* **1994**, *77*, 2789.
- [14] T. Luping, *Calibration of the Electrochemical Methods for the Corrosion Rate Measurements of Steel in Concrete*, Nordtest Project No. 1531-01, SP-Report 2002:25, SP Swedish National Testing and Research Institute, Sweden **2002**.
- [15] A. Poursae, *PhD Thesis*, University of Waterloo, Waterloo, Ontario, Canada **2007**.
- [16] H. Wojtas, *Corros. Sci.* **2004**, *46*, 1621.
- [17] C. Wagner, W. E. Traud, *Z. Elektrochem. Angew. Phys. Chem.* **1938**, *44*, 397.
- [18] U. Angst, M. Büchler, *Mater. Corros.* **2015**, *66*, 1017.
- [19] I. Martínez, C. Andrade, N. Rebolledo, L. Luo, G. De Schutter, *Corrosion* **2010**, *66*, 026001.
- [20] F. Mansfeld, *Corrosion* **1988**, *44*, 856.
- [21] W. Oelßner, F. Berthold, U. Guth, *Mater. Corros.* **2006**, *57*, 455.
- [22] P. J. M. Monteiro, H. F. Morrison, W. Frangos, *ACI Mater. J.* **1988**, *95*, 704.
- [23] J. Zhang, P. J. M. Monteiro, H. F. Morrison, *ACI Mater. J.* **2001**, *98*, 116.
- [24] C. Andrade, I. Martínez, *Corrosion* **2010**, *66*, 056001.
- [25] M. Keddani, X. R. Nóvoa, V. Vivier, *Corros. Sci.* **2009**, *51*, 1795.
- [26] C. Andrade, J. Sanchez, I. Martínez, N. Rebolledo, *Electrochim. Acta* **2011**, *56*, 1874.
- [27] J. Zhang, P. J. M. Monteiro, H. F. Morrison, *ACI Mater. J.* **2002**, *99*, 242.
- [28] J. Zhang, P. J. M. Monteiro, H. F. Morrison, M. Mancio, *ACI Mater. J.* **2004**, *101*, 273.
- [29] P. Ghods, A. Alizadeh, M. Salehi, *U. S. Patent No. 20170227481A1* **2017**.
- [30] A. Fahim, P. Ghods, R. Alizadeh, M. Salehi, S. Decarufel, *ASTM STP* **2018**, 1609.
- [31] A. Fahim, *MScE Thesis*, University of New Brunswick, Fredericton, NB, Canada **2018**.
- [32] *ASTM G1*, ASTM International, West Conshohocken, PA, **2017**.
- [33] P. Ghods, O. B. Isgor, *ACI Spec. Pub.* **2016**, *312*, 1.
- [34] *ASTM C192*, ASTM International, West Conshohocken, PA, **2016**.
- [35] B. Pradhan, B. Bhattacharjee, *Constr. Build. Mater.* **2009**, *23*, 2346.
- [36] G. K. Glass, *Corros. Sci.* **1995**, *37*, 597.
- [37] A. N. Scott, presented at *4th International Conference on Concrete Repair, Rehabilitation and Retrofitting (ICCR-4)*, Leipzig, Germany, 5-7 October, **2015**, pp. 61–65.
- [38] *ASTM G59*, ASTM International, West Conshohocken, PA, **2014**.
- [39] P. Rodriguez, J. A. Gonzalez, *Mag. Conc. Res.* **1994**, *46*, 91.
- [40] A. M. Hassanein, G. K. Glass, N. R. Buenfeld, *NDT E Inter.* **1998**, *31*, 265.
- [41] L. Dhoubi-Hachani, E. Triki, J. Grandet, A. Raharinaivo, *Cem. Conc. Res.* **1996**, *26*, 253.
- [42] E.G. Moffatt, *PhD Thesis*, University of New Brunswick, New Brunswick, Canada, **2016**.
- [43] J. Flis, A. Sehgal, D. Li, Y. Kho, S. Sabotl, H. Pickering, K. Osseo-Asare, P. D. Cady, *Condition Evaluation of Concrete Bridges Relative to Reinforcement Corrosion Volume 2: Method for Measuring the Corrosion Rate of Reinforcing Steel*. Strategic Highway Research Program, Washington DC **1993**.
- [44] O. K. Gepreags, C. M. Hansson, *J. ASTM Inter.* **2005**, *2*, 1.
- [45] M.E. Mitzithra, *PhD Thesis*, Universite De Toulouse, Toulouse, France, **2013**.
- [46] A. Poursae, C. M. Hansson, *Corros. Sci.* **2008**, *50*, 2739.
- [47] C. Andrade, J. A. González, *Mater. Corros.* **1978**, *29*, 515.
- [48] S. C. Kranc, A. A. Sagues, *J. Electrochem Soc.* **1997**, *144*, 2643.
- [49] J. A. González, A. Molina, M. L. Escudero, C. Andrade, *Corros. Sci.* **1985**, *25*, 917.
- [50] S. G. Millard, K. R. Gowers, R. P. Gill, *Brit. J. NDT* **1992**, *34*, 444.
- [51] F. Mansfeld, Y. Chen, H. Shih, *ASTM STP* **1990**, *1506*, 95.
- [52] B. A. Lambie, C. Brennan, J. Olofsson, O. Orwar, S. G. Weber, *Anal. Chem.* **2007**, *79*, 13771.

- [53] C. Andrade, L. Soler, C. Alonso, X. R. Nóvoa, M. Keddou, *Corros. Sci.* **1995**, *37*, 2013.
- [54] P. Gu, S. Elliott, R. Hristova, J. J. Beaudoin, R. Brousseau, B. Baldock, *ACI Mater. J.* **1997**, *94*, 385.
- [55] A. A. Pilla, *J. Electrochem. Soc.* **1970**, *117*, 467.
- [56] C. Christodoulou, C. I. Goodier, S. A. Austin, J. Webb, G. Glass, *Corros. Sci.* **2012**, *62*, 176.
- [57] Y. C. Lim, T. Noguchi, S. W. Shin, *ISIJ Int.* **2009**, *49*, 275.

How to cite this article: Fahim A, Ghods P, Isgor OB, Thomas MD. A critical examination of corrosion rate measurement techniques applied to reinforcing steel in concrete. *Materials and Corrosion*. 2018;1–16.

<https://doi.org/10.1002/maco.201810263>